Journal of Sensor Science and Technology
Vol. 33, No. 5 (2024) pp. 359-365
http://dx.doi.org/10.46670/JSST.2024.33.5.359
pISSN 1225-5475/eISSN 2093-7563

Advancements in Photoactivated Gas Sensors: A Review

Kichul Lee[1] and Inkyu Park[1,+]

Abstract

Chemiresistive semiconductor metal oxide (SMO) gas sensors detect gases based on resistance changes caused by gas adsorption/desorption on SMOs. These sensors have witnessed significant advancements with the development of microelectromechanical systems (MEMS) and nanotechnology. MEMS technology has facilitated mass production, miniaturization, and uniformity across sensors. Whereas, nanotechnology has contributed to the development of high-sensitivity gas sensing materials with large surface areas, catalytic coatings, and hybrid SMO junctions. However, SMOs require activation via external energy to overcome their bandgap energy and generate hot electron carriers, which are essential for high sensitivity and fast response/recovery times. Traditionally, embedded heaters have been used for this purpose; however, micro-and nano-heaters are plagued by high power consumption and low durability, which limit their use in mobile applications. Consequently, photoactivated gas sensing using light sources (e.g., lamps and LEDs) has garnered attention as an alternative approach. This study reviewed the progress from early lamp and LED-based research to recent studies on monolithic micro-LED (μLED) based gas sensors. μLED gas sensors facilitate room-temperature operation and ultra-low power consumption within the microwatt range. Consequently, they are highly suitable for integration into consumer electronics, smart farms, smart factories, and mobile gas sensors.

Keywords: Photoactivated gas sensors, Metal oxide, MEMS, Ultra-low-power, Micro-LED, Electronic nose

1. INTRODUCTION

Chemiresistive semiconductor metal oxide (SMO) gas sensors detect gases by measuring the change in resistance that occurs during the adsorption or desorption of gas molecules onto the SMO surface [1-4]. Recent developments in microelectromechanical systems (MEMS) and nanotechnology have significantly advanced the field of semiconductor gas sensors. MEMS technology has facilitated the mass production of miniature gas sensors on a wafer scale, reduced manufacturing costs, and improved sensor uniformity, thereby enhancing their applicability and adoption in real-world scenarios [5]. Nanotechnology has contributed to the development of highly sensitive gas sensing materials with large specific surface areas. Using nanostructures such as nanowires (NWs), nanotubes (NTs), nanospheres (NSs), and nanoflowers (NFs), the surface area can be maximized. This increases the frequency of contact with gas molecules, thereby improving the sensing performance [6-11]. The coating of SMO surfaces with multifunctional nanoparticles (NPs) such as gold (Au), platinum (Pt), and silver (Ag) as catalysts can significantly enhance the sensitivity and selectivity. The spillover effect, wherein active metal NPs adsorb gas molecules and transfer them to the adjacent SMO surface, greatly enhances the sensor sensitivity [10,12-17]. Furthermore, by applying hybrid structures of SMOs or coatings, bandgap engineering can be exploited to create semiconductor materials with the desired properties. The formation of junctions such as p-n or n-n junctions can control the electronic structure, electron mobility, and recombination, thus significantly improving the sensitivity and selectivity of gas sensors [8-21].

However, SMOs must be activated via external energy to overcome the bandgap energy (E_g) and generate hot electron carriers capable of facilitating redox reactions between the SMO surface and gas molecules. Traditionally, this activation has been realized using embedded micro-heaters, which thermally activate SMOs via Joule heating at high temperatures (typical range of 200–400°C). However, even the most advanced heating methods consume approximately 10 mW of power for operating voltages within 1–2 V [20,22,23]. Consequently, the expected usage time of a typical LiPo battery (1000 mAh) does not exceed one week.

[1]Department of Mechanical Engineering, Korea Advanced Institute of Science and Technology (KAIST)
Daejeon, 34141, Republic of Korea
[+]Corresponding author: inkyu@kaist.ac.kr
(Received: Aug. 26, 2024, Revised: Sep. 9, 2024, Accepted: Sep. 11, 2024)

Thus, the power consumption remains a significant issue for mobile gas sensors. To reduce power consumption, micro- and nano-heaters have been miniaturized, and suspended structures such as bridges and cantilevers have been proposed to minimize heat conduction to the surrounding substrate [24-26]. However, these structures are prone to thermal and mechanical durability issues owing to repeated heating and cooling cycles and external shocks. Consequently, heating methods are limited in terms of power consumption and durability when applied to mobile gas sensors.

Recently, photoactivated gas sensors that activate SMOs using light have gained attention owing to their low power consumption and low-temperature operation. This study examined the development of these sensors. This included starting from early studies using light sources such as lamps and LEDs to the latest research on monolithic micro-LED (μLED) based gas sensors [27,28]. μLED gas sensors can operate at room temperature and achieve ultra-low power consumption at the nano- and micro-watt levels. This renders them highly promising for applications in consumer electronics, smart farms, smart factories, and mobile gas sensors.

2. PHOTOACTIVATED GAS SENSORS

2.1 Photoactivated Sensors using External Light Sources

Early research on photoactivated gas sensors involved the use of external light sources such as LEDs and lamps to illuminate SMO-sensing materials from a distance of several centimeters, thereby inducing photoactivation. Although photoactivated gas sensors that utilize sunlight are self-powered, they are excluded from this discussion because of their limitations. These include being affected by the changing position of the sun, variations in illumination, weather conditions, and inoperability at night. The energy of photons contained in light of a specific wavelength can be calculated using the formula shown in eq. 1 below. Because the E_g values of SMOs commonly used in photoactivated gas sensors typically range between 2–4 eV [29], the wavelengths of light used in these sensors generally vary from the ultraviolet (UV) region to the red wavelength region (350–650 nm).

$$E(ev) = \frac{1240}{\lambda(nm)} \quad (1)$$

Although shorter wavelengths of light are more effective for activating SMOs, LEDs that emit UV light below 350 nm are less commonly used in practical applications. This is attributed to the increased defect density in the gallium nitride (GaN) layer, higher power consumption, and heat generation issues associated with short-wavelength UV LEDs.

In 2003, Yang et al. demonstrated a significant enhancement in CO gas sensitivity of more than 30 times. They simultaneously used a heater and a 367 nm UV LED to activate TiO_2 NPs [30]. A commercial LED was used with a power of 3.25 mW/cm^2 at a distance of 1 cm. The simultaneous application of heat of 200°C yielded an R_g/R_0 ratio of 87 for 300 ppm CO gas (Fig. 1 (a)). This study was not solely reliant on photoactivation; however, it demonstrated that reactivity was further improved when UV light was present in addition to traditional heating methods. In 2011, Zhai et al. detected formaldehyde using a 500 W 450 nm Xe lamp and a CdS NW/ZnO NSs composite structure [18]. In 2012, Zampetti et al. utilized a 390 nm UV LED (75 mW) with photoactivate electrospun Titania (TiO_2) nanofibers. This enabled the detection of NO_2 and NH_3 at ppb levels (Fig. 1 (b)) [31]. Jaisutti et al. used a 377 nm UV LED (5 mW/cm^2) and Na-doped ZnO to detect 100 ppm acetone with an R_g/R_0 ratio of 3.35 (Fig. 1 (c)) [6]. Numerous studies have reported the use of LEDs or lamps to photoactivate sensing materials for gas detection. However, when the light source is positioned away from the sensing material, the energy transfer efficiency is reduced because of energy losses during transmission, and power consumption

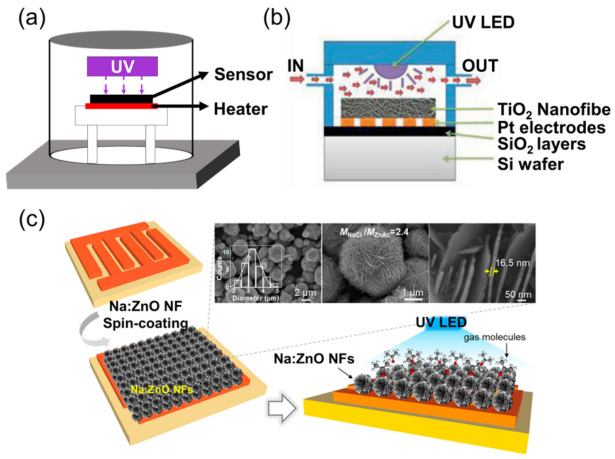

Fig. 1. Example of photoactivated gas sensors using a light source positioned several centimeters away from the sensing material. Owing to this separation, energy transfer efficiency is low, resulting in high power consumption. (a) 367 nm LED. (b) 390 nm LED. Reprinted with permission from Ref. [31] Copyright (2012) Elsevier. (c) 377 nm LED. Reprinted with permission from Ref. [6] Copyright (2017) American Chemical Society.

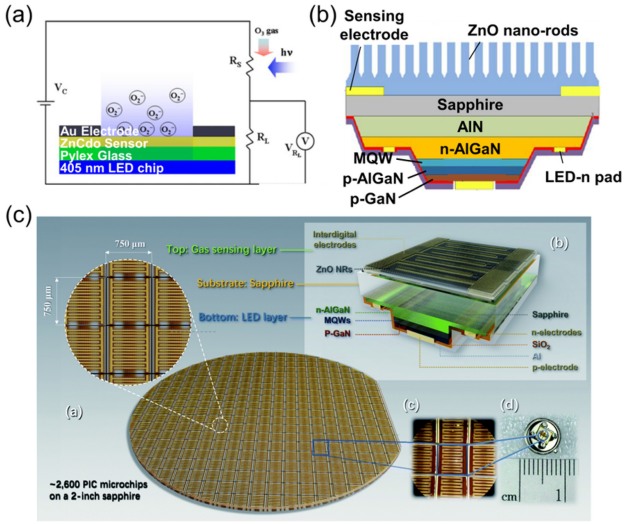

Fig. 2. Studies that have attempted to minimize the distance between the light source and sensing material. (a) ZnCdO thin film grown on a 405 nm LED via sputtering on a Pyrex substrate. Reprinted with permission from Ref. [35] Copyright (2013) Springer US. (b) and (c) ZnO nanorods grown via hydrothermal synthesis on a 280 nm deep UV flip-chip LED. Reprinted with permission from Ref. [37] and Ref. [36], respectively. Copyright (2020) American Chemical Society and Copyright (2021) Royal Society of Chemistry, respectively.

considerations are often neglected [7,32-34].

Thus, although the use of external light sources for photoactivation indicates an innovative departure from traditional heating methods by enabling room-temperature operation, it is plagued by limitations owing to its higher power consumption (75 mW to 500 W), compared to micro/nanoscale heaters (Joule heating methods).

Subsequent research focused on the reduction of the distance between the light source and sensing material with the aim of minimizing wasted light energy and power consumption. In 2013, Yu et al. developed an ozone gas sensor via the integration of ZnCdO thin films onto a Pyrex substrate placed directly on top of a 405 nm LED (Fig. 2 (a)) [35]. However, owing to the use of a commercial LED as the light source, the distance between the light source and the material remained separated by the thickness of the Pyrex substrate (several millimeters). Consequently, sub-microwatt-level gas detection could not be achieved (1.8 mW/cm^2). Zhang et al. utilized hydrothermal synthesis to deposit ZnO on a 280 nm deep UV flip-chip LED sapphire substrate to detect 500 ppb of NO_2 gas (Figs. 2 (b), (c)) [36,37]. However, because of the structure wherein UV light passes through the opaque sapphire substrate before reaching the ZnO sensing material, the power consumption remained at 3 mW, falling short of achieving sub-1 mW levels.

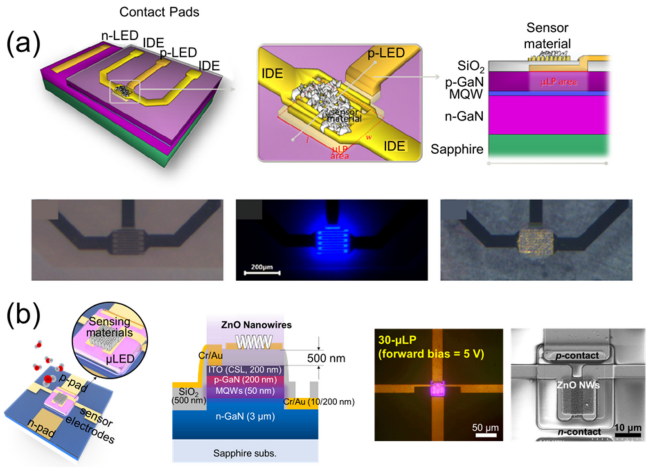

Fig. 3. Monolithic photoactivated gas sensor achieving microwatts power consumption. (a) 220 × 250 μm^2 LED with a wavelength of 455 nm. Reprinted with permission from Ref. [38] Copyright (2019) AIP Publishing. (b) 30 × 30 μm^2 μLED with a wavelength of 395 nm. Reprinted with permission from Ref. [40] Copyright (2020) American Chemical Society.

2.2 Monolithic Micro LED Gas Sensors with Microwatt-Level Power Consumption

Certain previous studies introduced in the earlier section experienced energy loss owing to the LED light pass through multiple layers prior to reaching the sensing material. However, since 2019, research has focused on monolithic gas sensors. Consequently, μLED is insulated insulation with a 1 μm SiO_2 layer and the placement of the sensing material directly on top. This design minimizes light loss and facilitates ultralow-power gas detection at sub-milliwatt levels. Markiewicz and Casals fabricated a 220 × 250 μm^2 455 nm blue LED (insulated with a 350 nm thick SiO_2 layer), with ZnO used as the sensing material [38,39] (Fig. 3 (a)). Consequently, they could detect 25 ppb NO_2 gas with a 94% response at a power consumption of 200 μW. Aiming to further reduce the size of the light source, Cho developed a 30 × 30 μm^2 390 nm UV LED, insulated with a 500 nm thick SiO_2 layer. Further, the used hydrothermally grown ZnO NWs to detect 1 ppm NO_2 gas with a 605% response at a power consumption of 184 μW [40] (Fig. 3 (b)). Consequently, through the development of a monolithic sensor platform wherein the light source and sensing material are integrated, the efficiency of the light energy transfer is maximized. This results in the creation of microwatt-level ultralow-power photoactivated gas sensors.

2.3 Micro LED Gas Sensors and Deep Learning-Based E-Nose Systems

In this section, we introduce the development of micro-LED gas sensors and deep-learning-based electronic nose (e-nose) systems. SMO-based chemiresistive gas sensors can often exhibit nonselective responses to chemically reactive gases. This is a critical issue that must be addressed to enable practical applications. An e-nose system mimics the human sense of olfaction using a sensor array that produces different responses to various gases coupled with deep-learning-based pattern recognition to selectively distinguish between gases. Although increasing the number of sensors in an e-nose system improves the accuracy, it also increases the overall volume and power consumption of the system. Therefore, the size and power consumption of individual sensors must be reduced to render μLED gas sensors suitable for this purpose.

Lee developed an e-nose system using two μLED gas sensors Each sensor had a different sensing material, and a convolutional neural network (CNN) algorithm, following the fabrication of a 395 nm UV μLED with a size of 50 × 50 μm^2. During sensor fabrication, a 1 μm thick double insulation SiO_2 layer was deposited to completely separate the sensor electrodes from the LED driving electrodes. This prevented electrical shorts even after the integration of various processing methods and materials on the LED [41] (Fig. 4 (a)). In addition, silver (Ag) and gold (Au) NPs with plasmonic properties were coated on the surface of In_2O_3 using e-beam evaporation, thus leveraging localized surface plasmon resonance (LSPR) to maximize hot electron carrier generation and significantly enhance gas sensitivity. Specifically, sensors coated with Ag and Au NPs exhibited more than 100 times greater sensitivity to NO_2 gas than the uncoated sensors. Consequently, the system achieved 99.3% accuracy in terms of identifying five different gas conditions: ethanol, acetone, nitrogen dioxide (NO_2), methanol, and normal air, and predicted gas concentration with 13.8% error, while consuming only 0.48 mW of power.

To further reduce the volume and power consumption of the e-nose, Cho and Lee developed a single-sensor based e-nose system and introduced pseudo-random illumination, wherein the μLED light was driven in random pulse patterns (Fig. 4 (b)) [42]. The gas sensor platform and sensing material remained the same, that is, a 395 nm UV μLED and Au NPs-coated In_2O_3 were used. When the μLED was driven with variable illumination, the photoactivity of the SMO and the number of hot electron carriers generated internally changed at every moment. This resulted in

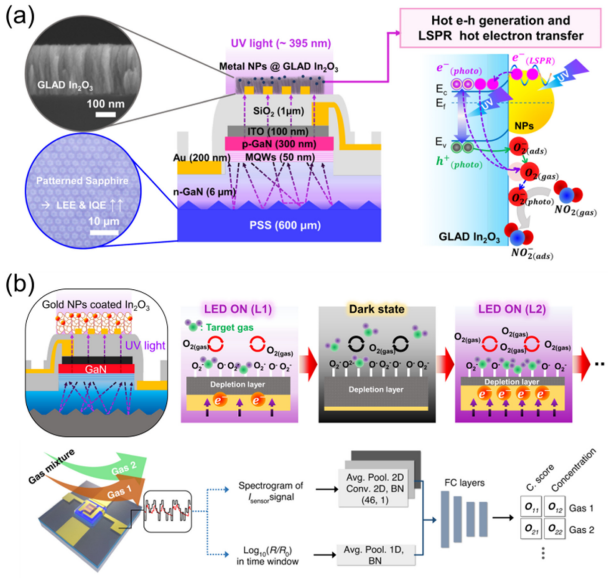

Fig. 4. Micro-LED and deep learning-based e-nose system. (a) System based on two μLED sensors (Au NPs-coated In_2O_3, Ag NPs-coated In_2O_3) Reprinted with permission from Ref. [41] Copyright (2023) American Chemical Society. (b) System based on a single μLED sensor (Au NPs-coated In_2O_3) and pseudo-random illumination. Reprinted with permission from Ref. [42] Copyright (2023) Springer Nature

unique transient response patterns depending on the type and concentration of the gas present in the ambient environment. Owing to variable driving, more diverse and multidimensional information can be obtained compared to driving a μLED with steady-state light intensity over the same period. The data collected through pseudo-random illumination were transformed into spectrogram data using a fast Fourier transform (FFT) and subsequently used as training data for the e-nose system model. Consequently, the system was found to successfully distinguish between five different single gases using only a single sensor. Moreover, it even predicted the type and concentration of gases in scenarios wherein two different gases (ethanol and methanol) were mixed. The μLED gas sensor-based e-nose system offers the potential to drastically reduce power consumption to less than one-hundredth of that of conventional Joule heating-based e-nose systems. This renders it highly promising for use as a ubiquitous environmental monitoring system with limited continuous power supply.

2.4 Nanowatt-Level Blue Micro LED Gas Sensors

In the previous sections, μLEDs with a 395 nm UV wavelength were used for photoactivate metal oxide sensing materials for gas detection. However, UV LEDs require the use of AlGaN to

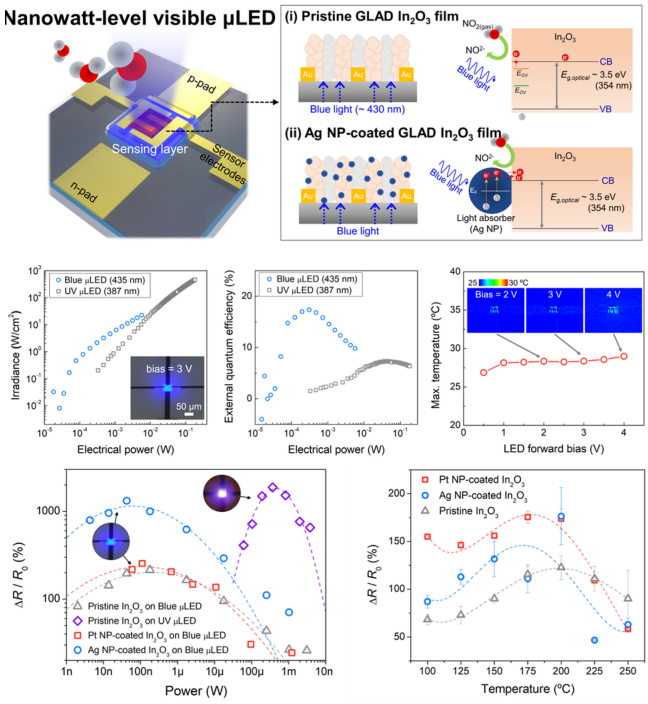

Fig. 5. Nanowatt-level gas sensing utilizing a 435 nm blue LED with stable GaN crystallinity and LSPR effects from silver NPs-coated In_2O_3. Reprinted with permission from Ref. [44] Copyright (2023) John Wiley and Sons.

produce UV wavelengths, consequently resulting in a high density of internal defects owing to the significant lattice and thermal mismatch between AlGaN and commonly used substrates such as sapphire. This renders the realization of good crystallinity in GaN challenging. Thus yielding a low external quantum efficiency (EQE) of less than 10%. In contrast, blue LEDs with wavelengths in the range of 430–470 nm used InGaN, which exhibited better crystallinity and fewer internal defects, thus achieving a higher EQE than UV LEDs [43]. In 2023, Cho et al. successfully utilized a 435 nm blue μLED with high light efficiency to achieve nanowatt-level (63 nW) gas detection (Fig. 5) [44]. The glancing angle deposited (GLAD) In_2O_3 was used as a gas sensing material, and to maximize the photoactivation by matching the 435 nm wavelength of the blue μLED with the absorbance of the sensing material. Here, Ag NPs were coated on the surface of the SMO using e-beam evaporation to leverage the LSPR effect. In addition, the optimal coating conditions for Ag NPs were identified. Further, experiments demonstrated that the improved gas sensitivity when coating SMO NPs in photoactivated gas sensors was attributable to the LSPR effect rather than catalytic effects. Moreover, based on IR (infrared) camera measurements, it was confirmed that the μLED maintained room temperature during light emission.

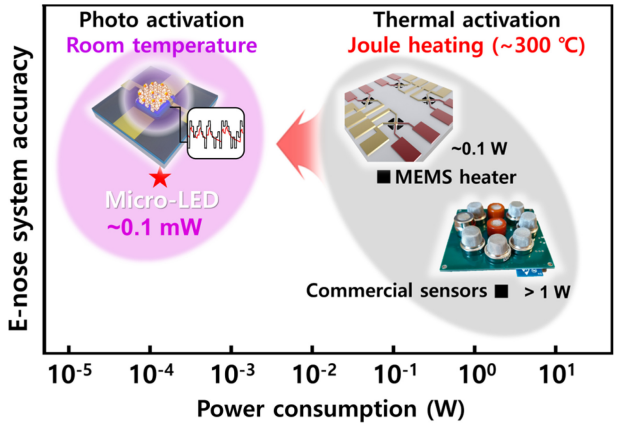

Fig. 6. Summary graph indicating the advantages of the micro LED-based sensor and e-nose system.

3. CONCLUSIONS

Thus, photoactivated gas sensors that utilize light energy to activate SMOs offer the advantage of room temperature operation and exhibit superior durability compared with suspended micro-heaters or nano-heaters. This is because they are not prone to fatigue failure caused by frequent heating and cooling cycles. Early research on photoactivated gas sensors faced challenges owing to the low energy transfer efficiency and high power consumption, which were attributable to the significant distance (several to tens of centimeters) between the light source and sensing material. However, recent advancements in monolithic sensors, wherein small light sources such as μLEDs are used and the distance between the light source and the sensing material is minimized to within 1 μm, have facilitated the reduction of power consumption by 2–3 orders of magnitude compared to heating methods. This capability of ultralow-power operation enabled stable long-term use even in battery-powered scenarios and allowed the light source to be controlled by the rendering the sensor functional regardless of the day, night, or weather conditions. Therefore, it is well suited for mobile gas sensing and can be applied in various fields, such as indoor air quality monitoring in home appliances, plant growth monitoring, smart factories, and industrial safety management.

Moreover, because LEDs are diodes, they do not require several minutes to cool or heat as in the case of heaters, and their ON/OFF switching is fast (within 1 ms). The theoretical lifespan of LEDs is approximately ten years. By driving the LED light in random pulse patterns, an e-nose system that minimizes the number of sensors used while still being able identifying each component of

the mixed gases can be developed (Fig. 6). In the future, the existing research will extend beyond SMOs to utilize other sensing materials, such as metal-organic frameworks (MOFs) and carbon nanomaterials (graphene, carbon nanotubes, etc.), thereby enabling the detection of various gases with high sensitivity and selectivity.

ACKNOWLEDGMENT

This work was supported by the National R&D Program through the National Research Foundation of Korea (NRF) funded by the Ministry of Science (Nos. 2021R1A2C3008742 and 2021M3H4A3A02099211).

REFERENCES

[1] D. Yang, M. K. Fuadi, K. Kang, D. Kim, Z. Li, and I. Park, "Multiplexed Gas Sensor Based on Heterogeneous Metal Oxide Nanomaterial Array Enabled by Localized Liquid-Phase Reaction", *ACS Appl. Mater. Interfaces*, Vol. 7, No. 19, pp. 10152-10161, 2015.

[2] D. Yang, D. Kim, S. H. Ko, A. P. Pisano, Z. Li, and I. Park, "Focused Energy Field Method for the Localized Synthesis and Direct Integration of 1D Nanomaterials on Microelectronic Devices", *Adv. Mater.*, Vol. 27, No. 7, pp. 1207-1215, 2015.

[3] D. Yang, I. Cho, D. Kim, M. A. Lim, Z. Li, J. G. Ok, M. Lee, and I. Park, "Gas Sensor by Direct Growth and Functionalization of Metal Oxide/Metal Sulfide Core-Shell Nanowires on Flexible Substrates", *ACS Appl. Mater. Interfaces*, Vol. 11, No. 27, pp. 24298-24307, 2019.

[4] A. Dey, "Semiconductor Metal Oxide Gas Sensors: A Review", *Mater. Sci. Eng. B*, Vol. 229, pp. 206-217, 2018.

[5] M. I. A. Asri, M. N. Hasan, M. R. A. Fuaad, Y. M. Yunos, and M. S. M. Ali, "MEMS Gas Sensors: A Review", *IEEE Sens. J.*, Vol. 21, No. 17, pp. 18381-18397, 2021.

[6] R. Jaisutti, M. Lee, J. Kim, S. Choi, T. J. Ha, J. Kim, H. Kim, S. K. Park, and Y. H. Kim, "Ultrasensitive Room-Temperature Operable Gas Sensors Using p-Type Na:ZnO Nanoflowers for Diabetes Detection", *ACS Appl. Mater. Interfaces*, Vol. 9, No. 10, pp. 8796-8804, 2017.

[7] Y. Mun, S. Park, S. An, C. Lee, and H. W. Kim, "NO_2 Gas Sensing Properties of Au-Functionalized Porous ZnO Nanosheets Enhanced by UV Irradiation", *Ceram. Int.*, Vol. 39, No. 8, pp. 8615-8622, 2013.

[8] J. M. Suh, D. Cho, S. Lee, T. H. Lee, J. W. Jung, J. Lee, S. H. Cho, T. H. Eom, J. W. Hong, Y. S. Shim, S. Jeon, and H. W. Jang, "Rationally Designed TiO_2 Nanostructures of Continuous Pore Network for Fast-Responding and Highly Sensitive Acetone Sensor", *Small Methods*, Vol. 5, No. 12, pp. 2100941(1)-2100941(10), 2021.

[9] N. T. Thang, L. T. Hong, N. H. Thoan, C. M. Hung, N. Van Duy, N. Van Hieu, and N. D. Hoa, "Controlled Synthesis of Ultrathin MoS_2 Nanoflowers for Highly Enhanced NO_2 Sensing at Room Temperature", *RSC Adv.*, Vol. 10, No. 22, pp. 12759-12771, 2020.

[10] Y. P. Sun, Y. F. Zhao, H. Sun, F. C. Jia, P. Kumar, and B. Liu, "Synthesis and Room-Temperature H_2S Sensing of Pt Nanoparticle-Functionalized SnO_2 Mesoporous Nanoflowers", *J. Alloys Compd.*, Vol. 842, p. 155813, 2020.

[11] J. Li, J. Xian, W. Wang, K. Cheng, M. Zeng, A. Zhang, S. Wu, X. Gao, X. Lu, and J. M. Liu, "Ultrafast Response and High-Sensitivity Acetone Gas Sensor Based on Porous Hollow Ru-Doped SnO_2 Nanotubes", *Sens. Actuators B Chem.*, Vol. 352, p. 131061, 2022.

[12] J. S. Jang, S. J. Kim, S. J. Choi, N. H. Kim, M. Hakim, A. Rothschild, and I. D. Kim, "Thin-Walled SnO_2 Nanotubes Functionalized with Pt and Au Catalysts via the Protein Templating Route and Their Selective Detection of Acetone and Hydrogen Sulfide Molecules", *Nanoscale*, Vol. 7, No. 39, pp. 16417-16426, 2015.

[13] D. Cho, J. M. Suh, S. H. Nam, S. Y. Park, M. Park, T. H. Lee, K. S. Choi, J. Lee, C. Ahn, H. W. Jang, Y. S. Shim, and S. Jeon, "Optically Activated 3D Thin-Shell TiO_2 for Super-Sensitive Chemoresistive Responses: Toward Visible Light Activation", *Adv. Sci.*, Vol. 8, No. 3, pp. 2001883(1)-2001883(10), 2021.

[14] G. Yuan, Y. Zhong, Y. Chen, Q. Zhuo, and X. Sun, "Highly Sensitive and Fast-Response Ethanol Sensing of Porous Co_3O_4 hollow Polyhedra via Palladium Reined Spillover Effect", *RSC Adv.*, Vol. 12, No. 11, pp. 6725-6731, 2022.

[15] Y. Xu, L. Zheng, C. Yang, X. Liu, and J. Zhang, "Highly Sensitive and Selective Electronic Sensor Based on Co Catalyzed SnO_2 Nanospheres for Acetone Detection", *Sens. Actuators B Chem.*, Vol. 304, p. 127237, 2020.

[16] N. Sui, X. Wei, S. Cao, P. Zhang, T. Zhou, and T. Zhang, "Nanoscale Bimetallic AuPt-Functionalized Metal Oxide Chemiresistors: Ppb-Level and Selective Detection for Ozone and Acetone", *ACS Sens.*, Vol. 7, No. 8, pp. 2178-2187, 2022.

[17] W. T. Koo, S. J. Choi, N. H. Kim, J. S. Jang, and I. D. Kim, "Catalyst-Decorated Hollow WO_3 Nanotubes Using Layer-by-Layer Self-Assembly on Polymeric Nanofiber Templates and Their Application in Exhaled Breath Sensor", *Sens. Actuators B Chem.*, Vol. 223, pp. 301-310, 2016.

[18] J. Zhai, L. Wang, D. Wang, H. Li, Y. Zhang, D. Q. He, and T. Xie, "Enhancement of Gas Sensing Properties of CdS Nanowire/ZnO Nanosphere Composite Materials at Room Temperature by Visible-Light Activation", *ACS Appl. Mater. Interfaces*, Vol. 3, No. 7, pp. 2253-2258, 2011.

[19] P. H. Phuoc, N. N. Viet, L. V. Thong, C. M. Hung, N. D. Hoa, N. Van Duy, H. S. Hong, and N. Van Hieu, "Comparative Study on the Gas-Sensing Performance of ZnO/SnO_2 External and ZnO–SnO_2 Internal Heterojunctions for Ppb H_2S and NO_2 Gases Detection", *Sens. Actuators B Chem.*, Vol. 334, p. 129606, 2021.

[20] H. Long, S. Turner, A. Yan, H. Xu, M. Jang, C. Carraro, R. Maboudian, and A. Zettl, "Plasma Assisted Formation of 3D Highly Porous Nanostructured Metal Oxide Network on Microheater Platform for Low Power Gas Sensing", *Sens.*

Actuators B Chem., Vol. 301, p. 127067, 2019.

[21] W. T. Koo, S. J. Choi, S. J. Kim, J. S. Jang, H. L. Tuller, and I. D. Kim, "Heterogeneous Sensitization of Metal-Organic Framework Driven Metal@Metal Oxide Complex Catalysts on an Oxide Nanofiber Scaffold Toward Superior Gas Sensors", *J. Am. Chem. Soc.*, Vol. 138, No. 40, pp. 13431-13437, 2016.

[22] M. Kang, I. Cho, J. Park, J. Jeong, K. Lee, B. Lee, D. Del Orbe Henriquez, K. Yoon, and I. Park, "High Accuracy Real-Time Multi-Gas Identification by a Batch-Uniform Gas Sensor Array and Deep Learning Algorithm", *ACS Sens.*, Vol. 7, No. 2, pp. 430-440, 2022.

[23] B. Lee, I. Cho, M. Kang, D. Yang, and I. Park, "Thermally/Mechanically Robust Anodic Aluminum Oxide (AAO) Microheater Platform for Low Power Chemoresistive Gas Sensor", *J. Micromech. Microeng.*, Vol. 33, No. 8, p. 085011, 2023.

[24] G. Meng, F. Zhuge, K. Nagashima, A. Nakao, M. Kanai, Y. He, M. Boudot, T. Takahashi, K. Uchida, and T. Yanagida, "Nanoscale Thermal Management of Single SnO_2 Nanowire: Pico-Joule Energy Consumed Molecule Sensor", *ACS Sens.*, Vol. 1, No. 8, pp. 997-1002, 2016.

[25] D. Xie, D. Chen, S. Peng, Y. Yang, L. Xu, and F. Wu, "A Low Power Cantilever-Based Metal Oxide Semiconductor Gas Sensor", *IEEE Electron Device Lett.*, Vol. 40, No. 7, pp. 1178-1181, 2019.

[26] T. Kim, W. Cho, B. Kim, J. Yeom, Y. M. Kwon, J. M. Baik, J. J. Kim, and H. Shin, "Batch Nanofabrication of Suspended Single 1D Nanoheaters for Ultralow-Power Metal Oxide Semiconductor-Based Gas Sensors", *Small*, Vol. 18, No. 48, pp. 1-14, 2022.

[27] R. Kumar, X. Liu, J. Zhang, and M. Kumar, "Room-Temperature Gas Sensors Under Photoactivation: From Metal Oxides to 2D Materials", *Nano Micro Lett.*, Vol. 12, No. 164, pp. 1-37, 2020.

[28] J. M. Suh, T. H. Eom, S. H. Cho, T. Kim, and H. W. Jang, "Light-Activated Gas Sensing: A Perspective of Integration with Micro-LEDs and Plasmonic Nanoparticles", *Mater. Adv.*, Vol. 2, No. 3, pp 827-844, 2021.

[29] O. Ishchenko, V. Rogé, G. Lamblin, D. Lenoble, and I. Fechete, "TiO_2, ZnO, and SnO_2-Based Metal Oxides for Photocatalytic Applications: Principles and Development", *Comptes Rendus. Chim.*, Vol. 24, No. 1, pp. 103-124, 2021.

[30] T. Y. Yang, H. M. Lin, B. Y. Wei, C. Y. Wu, and C. K. Lin, "UV enhancement of the gas sensing properties of nano-TiO_2", *Rev. Adv. Mater. Sci.*, Vol. 4, No. 1, pp. 48-54, 2003.

[31] E. Zampettia, A. Bearzotti, and A. Macagnano, "UV Assisted Chemical Sensor Based on Electrospun Titania Nanofibers Working at Room Temperature", *Procedia Eng.*, Vol. 47, pp. 912-915, 2012.

[32] J. Azizi Jarmoshti, A. Nikfarjam, H. Hajghassem, and S. M. Banihashemian, "Visible Light Enhancement of Ammonia Detection Using Silver Nanoparticles Decorated on Reduced Graphene Oxide", *Mater. Res. Express*, Vol. 6, No. 6, p. 066306, 2019.

[33] S. Park, M. Kim, Y. Lim, D. H. Oh, J. Ahn, C. Park, S. Woo, W. C. Jung, J. Kim, and I. D. Kim, "Dual-Photosensitizer Synergy Empowers Ambient Light Photoactivation of Indium Oxide for High-Performance NO_2 Sensing", *Adv. Mater.*, Vol. 36, No. 24, pp. 1-14, 2024.

[34] X. Yan, Y. Wu, R. Li, C. Shi, R. Moro, Y. Ma, and L. Ma, "High-Performance UV-Assisted NO_2 Sensor Based on Chemical Vapor Deposition Graphene at Room Temperature", *ACS Omega*, Vol. 4, No. 10, pp. 14179-14187, 2019.

[35] J. H. Yu, H. J. Yang, H. S. Mo, T. S. Kim, T. S. Jeong, C. J. Youn, and K. J. Hong, "Sensing Mechanism and Behavior of Sputtered ZnCdO Ozone Sensors Enhanced by Photons for Room-Temperature Operation", *J. Electron. Mater.*, Vol. 42, No. 4, pp. 720-725, 2013.

[36] X. X. Wang, S. Zhang, Y. Liu, J. N. Dai, H. Y. Li, and X. Guo, "Light-Excited Chemiresistive Sensors Integrated on LED Microchips", *J. Mater. Chem. A*, Vol. 9, No. 30, pp. 16545-16553, 2021.

[37] S. Zhang, H. Li, X. Wang, Y. Liu, J. Dai, and C. Chen, "Highly Integrated in Situ Photoenergy Gas Sensor with Deep Ultraviolet LED", *ACS Omega*, Vol. 5, No. 17, pp. 9985-9990, 2020.

[38] N. Markiewicz, O. Casals, C. Fabrega, I. Gràcia, C. Cané, H. S. Wasisto, A. Waag, and J. D. Prades, "Micro Light Plates for Low-Power Photoactivated (Gas) Sensors", *Appl. Phys. Lett.*, Vol. 114, No. 5, pp. 1-6, 2019.

[39] O. Casals, N. Markiewicz, C. Fabrega, I. Gràcia, C. Cane, H. S. Wasisto, A. Waag, and J. D. Prades, "A Parts per Billion (Ppb) Sensor for NO_2 with Microwatt (μW) Power Requirements Based on Micro Light Plates", *ACS Sens.*, Vol. 4, No. 4, pp. 822-826, 2019.

[40] I. Cho, Y. C. Sim, M. Cho, Y. H. Cho, and I. Park, "Monolithic Micro Light-Emitting Diode/Metal Oxide Nanowire Gas Sensor with Microwatt-Level Power Consumption", *ACS Sens.*, Vol. 5, No. 2, pp. 563-570, 2020.

[41] K. Lee, I. Cho, M. Kang, J. Jeong, M. Choi, K. Y. Woo, K. J. Yoon, Y. H. Cho, and I. Park, "Ultra-Low-Power E-Nose System Based on Multi-Micro-LED-Integrated, Nanostructured Gas Sensors and Deep Learning", *ACS Nano*, Vol. 17, No. 1, pp. 539-551, 2023.

[42] I. Cho, K. Lee, Y. C. Sim, J. S. Jeong, M. Cho, H. Jung, M. Kang, Y. H. Cho, S. C. Ha, K. J. Yoon, and I. Park, "Deep-Learning-Based Gas Identification by Time-Variant Illumination of a Single Micro-LED-Embedded Gas Sensor", *Light Sci. Appl.*, Vol. 12, No. 1, p. 95, 2023.

[43] Z. Chen, S. Yan, and C. Danesh, "MicroLED Technologies and Applications: Characteristics, Fabrication, Progress, and Challenges", *J. Phys. D Appl. Phys.*, Vol. 54, No. 12, p. 123001, 2021.

[44] I. Cho, Y. C. Sim, K. Lee, M. Cho, J. Park, M. Kang, K. S. Chang, C. B. Jeong, Y. H. Cho, and I. Park, "Nanowatt-Level Photoactivated Gas Sensor Based on Fully-Integrated Visible MicroLED and Plasmonic Nanomaterials", *Small*, Vol. 19, No. 27, pp. 1-10, 2023.